Visualization of Multimodality Cardiac Imagery

JOHN W. PEIFER, MEMBER, IEEE, NOBERTO F. EZQUERRA, CHARLES DAVID COOKE, RAKESH MULLICK, STUDENT MEMBER, IEEE, L. KLEIN, M. ERIC HYCHE, ERNEST V. GARCIA, MEMBER, IEEE

Abstract—**A large number of clinically important and medically difficult decisions in diagnostic radiology involve interpreting the information derived from multiple imaging modalities. This is especially true in the assessment of heart disease, wherein at least two types of image information are generally required prior to deciding on the course of action: structural information describing coronary vessel anatomy and functional information related to heart muscle physiology. This paper will present and discuss the methods and results associated with a research program aimed at quantifying and visualizing the unified anatomic and physiologic information obtained from these complementary imaging modalities. The discussions will emphasize the reconstruction, processing, and visualization of three-dimensional cardiovascular structure, including the procedures and results obtained from phantom and patient studies.**

I. INTRODUCTION

ONE OF THE MOST important concerns of modern health care is the prevention, detection, and treatment of heart disease. Clinical decisions regarding this vital health care problem, such as decisions concerning a patient's diagnosis, therapy, and prognosis, largely depend on the accurate and reliable assessment of the extent and severity of coronary artery disease (CAD). To a great extent, this assessment is based on interpreting the information contained in various radiological images of the cardiovascular system, and therefore, those images become an integral part of the overall medical decision-making process. However, there are a number of limitations, medical considerations, and technical complexities associated with the task of making interpretive decisions based on this imagery. For instance, the information is usually acquired in two dimensions, although interpretation can be facilitated through three-dimensional (3-D) presentation. In addition, the information is typically reviewed through subjective, visual observation, rather than accurately characterized quantitatively. Furthermore, clinical interpretation relies on vast quantities of diverse types of information (image-based as well as nonimage data), thereby making decision-making tasks information intensive. Moreover, the informational content of the imagery may not be fully exploited, especially if the images corresponding to different modalities are considered separately rather than in a unified manner. To help overcome these and other limitations and complexities, the visualization methodology described herein is aimed at facilitating and enhancing the clinical decision-making process by incorporating approaches and techniques from computer vision, image processing, and computational graphics. The central concept underlying the methodology is that visual information derived from multiple imaging modalities can be unified and visualized in a three- or four-dimensional, interactive computer model, and that this visualization model can assist diagnosticians in interpreting large amounts of multidimensional information in a relatively easy, quick, and reliable manner.

It would be worthwhile to briefly examine a number of technical issues in order to more fully appreciate how a computer-based visualization methodology can aid in the overall clinical decision-making process. Prognosis in patients with CAD is determined [1]–[6] primarily by two factors: 1) the severity and extent of atheromatous obstruction (a blockage or stenotic lesion) in the coronary arterial circulation, and 2) the degree of left ventricular impairment (i.e., impairment of the heart muscle, or myocardium). Arterial vasculature and myocardial structures of interest are schematically depicted in Fig. 1. The two aforementioned factors can be viewed as lesions and impairment occurring in the arteries and tissue depicted in Fig. 1. To obtain information regarding these two factors, different clinical procedures are involved: for assessment of the extent and severity of atheromatous obstruction, the "gold standard" remains coronary arteriography [7], wherein contrast-enhancing injections into the coronary arteries allow the measurement of luminal diameter narrowing and the site of the stenosis; for assessment of the extent and severity of myocardial ischemia (inadequate blood supply to tissue) and infarction (dead or dying tissue), the "gold standard" remains myocardial perfusion tomography [8]–[12], employing techniques such as single-photon emission tomography (SPECT) using thallium-201 (Tl-201) or technicium-99 (Tc-99m-MlBl). In essence, coronary arteriography yields anatomical or structural information, while myocardial perfusion tomography provides physiological or functional information. Hence, an accurate assessment of the extent and severity of CAD ideally requires the integra-

Manuscript received August 2, 1989; revised March 1, 1990. This work was supported in part by Grants 1 RO1 HL42052-01 from the National Institutes of Health and R 29 LM04692 from the National Library of Medicine. One of the authors (Hyche) was supported by a Graduate Fellowship from the Office of Naval Research.

J. W. Peifer, N. F. Ezquerra, R. Mullick, and M. E. Hyche are with the Georgia Institute of Technology, Atlanta, GA 30332.

C. D. Cooke and L. Klein are with the School of Medicine, Emory University, Atlanta, GA 30322.

IEEE Log Number 9036234.

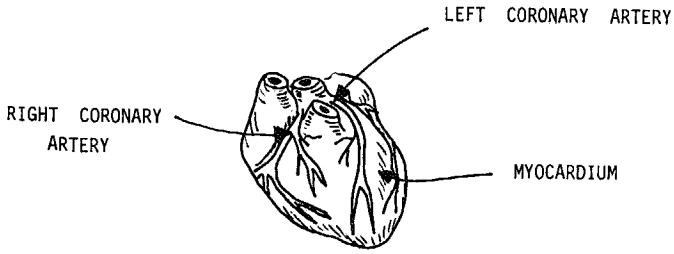

Fig. 1. Illustration of arterial vasculature and myocardial structures of interest.

tion of anatomical and physiological information obtained independently from these two imaging modalities. In practice, however, this information is seldom formally integrated or accurately quantified: rather, a mental "integration" is performed by the physician by visually studying a series of (mostly two-dimensional) images, and subsequently inferring or estimating spatial and temporal relationships from these images. To illustrate the level of difficulty associated with making such decisions, consider Figs. 2 and 3.

Fig. 2 shows a patient's coronary angiogram viewed from two different angles while Fig. 3 shows a series of tomographic slices depicting a patient's left ventricular perfusion distribution from the base to the apex of the heart. Fig. 2 thus shows vascular structure while Fig. 3 shows the perfusion distribution for different "slices" of the heart. Figs. 2 and 3 are typical of the type of imagery that is used in clinical decision-making for assessing the extent and severity of CAD. Clearly, mentally reconstructing and interpreting the information contained in Figs. 2 and 3 represents a formidable visualization task! Therein lies the overall objective of the methodology discussed in this paper: to aid in more easily characterizing and interpreting visual information, ideally "transforming" Figs. 2 and 3 into a meaningful, patient-specific version of Fig. 1, thereby improving the quantitative as well as qualitative assessment of anatomic and physiologic factors associated with coronary artery disease.

In particular, the primary goals of the visualization methodology are to improve the detection and evaluation of disease by combining the information from the two aforementioned modalities into a unified, computer-based 3-D model of structure and function. Through this unified model, the physician cannot only visualize the possible interrelationships between arterial circulation and myocardial impairment, but can also obtain a quantitative assessment of these relationships. For instance, a physician may use the model to quantitate and visualize the impact of a specific stenoic lesion on the blood supply associated with a particular region of the myocardium, and thus be able to more objectively determine how to proceed in the treatment of the patient. These are distinct and highly useful clinical advantages since even experienced physicians may not be able to easily visualize the 3-D geometry of the coronaries and how they relate to myocardial function.

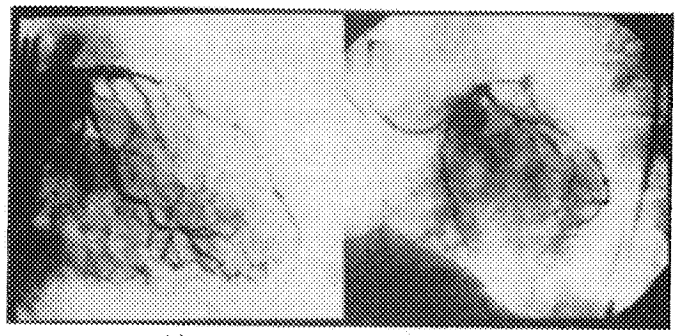

(a) (b)

Fig. 2. Two angiographic views: (a) RAO and (b) LAO views of a patient's left coronary artery.

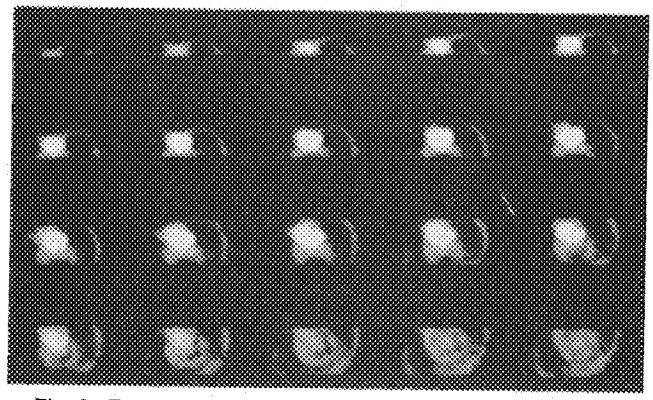

Fig. 2. Tomographic slices of a patient's perfusion distribution.

The task of objectively and accurately integrating and visualizing the multimodality information through a unified 3-D model requires several complex steps. The 3-D arterial structure must be reconstructed from a only few two-dimensional (2-D) angiographic views such as the ones shown in Fig. 2. Vascular dimensions, including stenotic lesions, must subsequently be extracted, located, quantified, modeled, and visualized to produce accurate 3-D representations of vascular structure. The perfusion distribution is originally obtained three-dimensionally (i.e., tomographically), but a model must also be generated to represent different perfusion levels three-dimensionally, and subsequently this information must be integrated with the vascular structures. In addition to these considerations, visualization procedures should also allow for user interaction, such as manipulation of the imagery, in order to further enhance the interpretive and decision-making processes.

To address these considerations, the visualization methodology is based on a computer model that organizes the multimodality information into a hierarchical data structure to more easily represent the patient-specific arterial tree in 3-D, and subsequently superimposes this tree onto a 3-D myocardial model that is color coded to represent relative perfusion levels. Vascular structures are modeled as collections of connected conical segments defined by vessel midpoints and diameters, while myocardial perfusion distributions are modeled as ellipsoidal 3-D surfaces. Once the model is created, it may be dis-

played in any arbitrary orientation as well as in animated sequences to enhance visualization. Quantitative information regarding stenotic dimensions and perfusion distributions can be obtained numerically to support the objective analysis of the graphical 3-D display. The remainder of this paper is devoted to a discussion of these techniques, accompanied by numerous graphical illustrations of results obtained from phantom and patient studies.

The paper is organized to reflect the salient characteristics of the methodology: Section II is devoted to quantification and visualization of anatomical information, including measured errors, Section III deals with quantification and visualization of physiological information, Section IV discusses visualization of the integrated modalities, while Section V provides a summary of results and future research directions. It should be pointed out that the discussions and results contained herein represent preliminary efforts in a multiyear research program, and that the present discussions amplify and emphasize visualization aspects of the methodology; previous publications [13]–[15] emphasize different aspects of this ongoing research.

II. Quantification and Visualization of Anatomical Information

The problem of quantifying and visualizing 3-D vascular structure from limited views remains one of the most difficult and interesting problems in biomedical research. To date, no scheme has been fully developed to take into account the particular morphology of the stenosis visualized. A number of studies [16]–[20] report on attempts to use biplaner projections to calculate luminal diameter narrowing from 3-D representations of parts of the vascular structure. These methods rely on operator-selected identification of stenotic sites. Other semiautomated approaches [21]–[23] use operator-selected landmarks (e.g., vessel bifurcations) to reconstruct 3-D or 4-D representations of the entire coronary arterial tree.

The limited view backprojection procedure under development in our research is illustrated in Fig. 4. Basically, the procedure requires specific knowledge of the system geometry (relative positions and orientations of X-ray sources and image planes) and identification of corresponding points in the biplanar projections (sometimes referred to as stereo projections). Ideally, the projection lines from the two sources S_1 and S_2, passing through a specific point in 3-D space, would intersect at that point and subsequently map onto the two views (view 1 and 2) as two distinct points on these planes. Thus, by backprojecting these projection points to their respective sources, the desired 3-D coordinate information for this intersection point can be found. In practice, however, numerous complications arise: there are errors in the known geometry of the data-acquisition system; the scattering, attenuation, and divergence of the X-ray beams corrupt the information; the arterial structure itself is inherently complex, and may not be easily defined by a finite set of

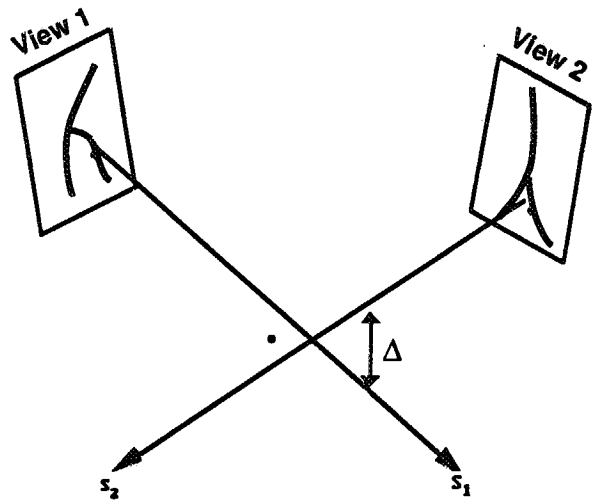

Fig. 4. Back projected lines from biplanar images. Δ is the shortest line segment separating back projection lines in 3-D space. The dot indicates the location of the true backprojection solution, estimated to be at the midpoint of the line segment Δ.

points; corresponding points in the two views are sometimes not easily detected and identified; and there is limited information when only a few views are available. The visualization methodology, as discussed subsequently, is aimed at taking into account these considerations.

Interactive Data Manipulation and Structure

Since a major portion of the visualization approach deals with reconstructing the information contained in the biplaner views, the data structure and programmatic operations have been developed to allow for user intervention during the reconstruction procedure. The data structure and programmatics are also designed to allow for the visualization of either specific vessels or branches (in 2-D or 3-D), or of entire vasculature. To accomplish these and other goals, the organization of the data structures, algorithmic procedures, and logical flow are designed hierarchically and modularly in nature. This is done for several reasons: the anatomical structure of the coronary tree is inherently hierarchical in nature, and this organization can thus be preserved in the data structure. In addition, reasoning strategies to visually detect and identify features of medical interest can also be more naturally represented in a hierarchical fashion. And, through modularity, different tasks can be separated and modified independently.

The primary tasks related to data manipulation include initialization, detection of vascular structures in multiple views, backprojection to 3-D solutions, 3-D model creation, and generation of reports of backprojection errors. The two- and three-dimensional geometries are retained in the data structure, which is designed to facilitate using additional views (i.e., more than two views, if available), from different geometries, and at different times (i.e., various frames throughout the cardiac cycle). A data hierarchy organizes the arterial geometry in each of the 2-D projections as well as in the final backprojected solution. In this hierarchy, an arterial structure is defined as a con-

tinuous arrangement of branches connected by bifurcation nodes, in much the same manner as the natural anatomy of the arterial tree occurs. The data structure is designed as a linked list to allow for branches of varying lengths, although once a branch has been defined in the first view, the number of points in that branch is fixed and cannot be changed in the other view (otherwise, some points would not have corresponding projections). A diagram of the database structure is shown in Fig. 5. The hierarchical order begins with a tree's "root" and a pointer to the first branch. (To maintain consistency throughout the structure, the starting location in the arterial structure, called the root, is defined to be a bifurcation point.) At each level below the root, branches and subbranches are described. The branch structure contains pointers describing bifurcations locations at either end of the current branch of interest, as well as pointers to the next branch. The branch structure also describes the number of, and geometry associated with, vessel cross sectional areas for which information is obtained (i.e., vessel centerpoint, vessel cross-sectional area, and orientation of this area). These vessel cross sectional areas or "slices" have pointers to groups containing additional information gathered during reconstruction, such as 2-D information regarding the biplaner views and 3-D information describing back-projection solutions.

Thus, through a network of bifurcations and branch pointers, the arterial structure is spawned, and the related 2-D and 3-D information is retained. The hierarchical data structure offers numerous practical advantages. For instance, this organizational framework allows for efficient traversing of the database, and provides a naturally recursive path through an arbitrary arterial structure. The structure also provides a framework for ensuring branch connectivity, simplifies smoothing across branches, and allows the reconstruction to be delayed until all 2-D projections have been acquired for the entire tree. In addition, anatomic information contained in the structure can be used for analysis of individual branches, as well as allowing for iterative improvement of the information through user interaction and manipulation of the data. Moreover, the tasks of graphical display and visualization can be more efficiently handled through this type of organization.

Data Acquisition, Corrections, and Transformations

As previously stated, a 3-D representation of the coronary arteries is obtained by reconstructing the information contained in a limited number of angiographic images. To generate the images clinically, a contrast agent is injected, through catheterization, into each of the left and right coronary arteries at different times, such that the two structures can be studied separately. For optimal reconstruction purposes, a pair of angiographic views must be simultaneously acquired since the heart beats and thus the arterial structure changes in time. Current protocols limit the number of simultaneous views that are actually collected at any point in the cardiac cycle to two, in order to

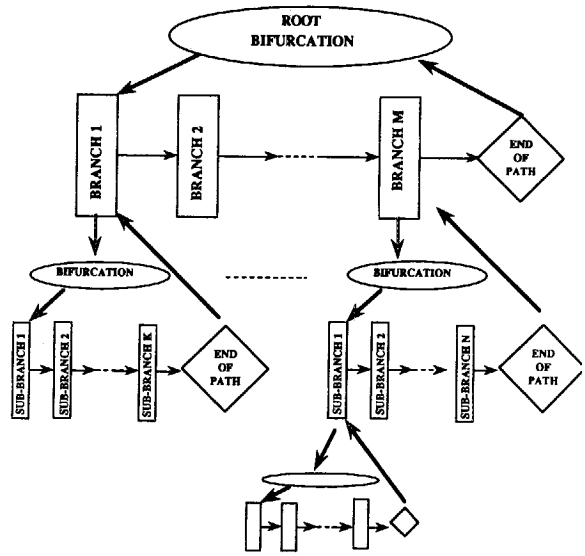

Fig. 5. Overview of data structure.

minimize patient radiation. As a result, the reconstruction problem is significantly different from tomographic reconstruction where information is obtained at many angles over large angular segments and object location is calculated from weighted and filtered line integrals.

Our methodology is designed to take into account any number of views as well as any arbitrary orientation geometries for the views. The reconstruction procedure requires accurate knowledge of the positions and orientations of the X-ray sources and image intensifiers. The digital images are obtained from a Philips Digital Angiographic System residing at the Emory University Hospital and routinely used in clinical practice. For this system, the two X-ray sources illuminate two image intensifiers identified as the right anterior oblique (RAO) view and the left anterior oblique (LAO) view. The face of each image intensifier is assumed to be orthogonal to the centerline of the beam from the corresponding X-ray source; the distance from source to intensifier, as well as viewing angles, may vary. An important feature of this type of angiographic system is that the beam centerlines for the RAO and LAO views always intersect at a common point, called the isocenter, regardless of the combination of intensifier distances and orientations. The centerline of the beam from the source also projects to the center of the image intensifier. The isocenter can thus be considered to be at the center of concentric spheres, and line segments of arbitrary length and orientation may be drawn through the isocenter.

In general, an attempt is made to position the patient's heart close to the isocenter such that the same arterial structure can be visualized from the RAO and LAO views. The RAO and LAO intensifiers and sources may be rotated electromechanically through a limited range of angles about the isocenter. In terms of patient data acquisition, Fig. 6 shows a diagram of these rotation angles with respect to the patient. The biplane system is designed to acquire images for a patient lying on his back, as illus-

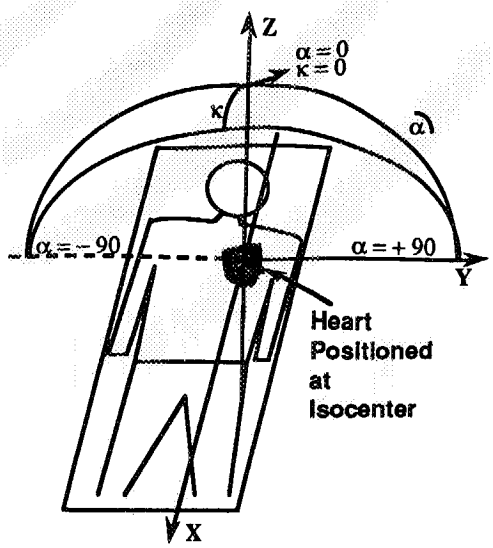

Fig. 6. Coordinate system and angle convention for biplane system and reconstruction. κ is positive in caudal direction and negative in cranial direction.

trated in Fig. 6, and as the names imply, RAO views are primarily limited to the right anterior side of the patient (whose heart is positioned at the isocenter), and LAO views are limited to the left anterior side of the patient. The orientations of the RAO and LAO views are defined by pairs of angles in a spherical coordinate system. Unlike distances, which require special calibration measurements, the values for these angles are provided by the angiographic system. The angles are defined as rotation (α) and skew (κ) angles, as in Fig. 6, which also illustrates a right-handed Cartesian coordinate system centered at the isocenter. The skew angle (κ) thus defines a plane rotated about the y axis, in which the rotation angle (α) is measured; the value of k is measured from the z axis. The reconstruction procedure, discussed in the next section, requires knowledge of these angles, although it does not require that the two biplane views be orthogonal.

In addition to defining the positions and angles of the image intensifiers, the relationship between the actual acquisition geometry and the displayed image must also be specified. As described earlier, images are assumed to be centered, on and orthogonal to, the centerline of the X-ray beam. However, the displayed images are inverted from the perspective of the X-ray source and, in addition, the images are displayed with the head-to-feet axis of the patient forming the vertical dimension of the image (to accommodate clinical convention). Corrections for these rotations and inversions are performed prior to reconstruction. A final correction deals with nonlinear distortions of the image. In the process of data acquisition, several distortions are incurred as a result of nonlinearities and inaccuracies inherent in X-ray transmission and acquisition [24]. A primary distortion for which we corrected is the so-called "pin cushion" effect. The pincushion distortion is caused by the slight curvature of the image intensifier screen and has the visual effect of parabolically warping the image radially away from the center. The approach taken for pincushion distortion correction is similar to well-known procedures set forth by other investigators [21].

Vascular Structure Detection

Prior to 3-D backprojection, the arterial structure in the 2-D projected views is defined. Transformations are defined to map 2-D image coordinates in the biplaner view pairs into 3-D coordinates of the projected point, based on the rotation and skew angles and on the distance to the image intensifier. More specifically, the location of the center of the vessel and the width of the vessel are obtained from each view of the biplane pair; these three points (center and two edge points) are specified at selected locations in the vascular structure with sufficient resolution to quantify vessel dimensions and stenotic lesions. As proposed by other authors [19], the assumption is made that the cross-sectional area of the vessel can be approximated by a circle.

At present, the detection procedure requires that the operator select or "sample" the center points of a branch in a 2-D projection, and subsequently edge boundaries are automatically sought from this selected point. The starting point in the procedure is the root bifurcation (which, in terms of anatomical landmarks, would correspond to the left main of the left coronary arterial tree, for instance). As vessel center points are obtained for the coronary tree, the 2-D and 3-D points corresponding to individual branches are stored in the hierarchical data structure, as previously discussed.

The procedure is illustrated in Fig. 7, showing operator-selected vessel center points and line segments along which edges are detected. Edge detection is performed on these line segments to locate the "left" and "right" edges for each chosen center point. Once these edges are obtained, the manually selected center point is "corrected" by redefining it as the midpoint between the detected edge points. The edge detection scheme searches for edges along a segment perpendicular to the vessel at the center point. Once the end points of the profile of search are determined, the Bresenham graphics line generation algorithm [25] is employed to generate a list of the image pixels lying along this profile.

For detecting vessel edges in angiographic images, a number of procedures have been proposed which are based on analysis of image intensity and contrast density distributions [21], [26], [27]. It is well known that common operators, such as gradient, Laplacian, Roberts, Sobel, Davies, and Prewitt operators [28], [29] do not give sufficiently consistent results over a full range of images due to variations in background levels, vessel overlap, and overall structural complexities. Hence, the detection process must be dynamic or adaptive, and "guided" by constraints and prior knowledge. After performing a number of tests with various combinations of the aforementioned techniques, it was decided to detect the "left" and "right" edges along the determined intensity profile by means of the entropy operator [30] preceded by histogram equalization and by Laplacian-of-a-Gaussian (LoG) operators [31].

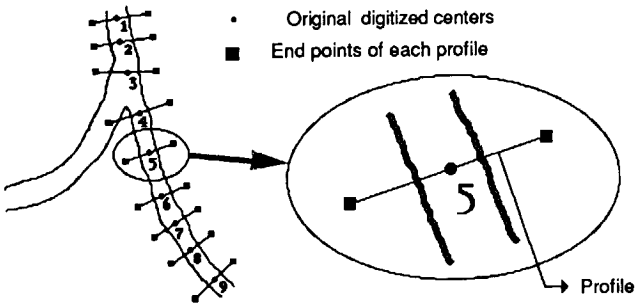

Fig. 7. Diagram illustrating edge detection procedure, including midpoint selection and profile generation.

It is noteworthy that the results of the edge detection procedures just described provide not only the 2-D information necessary to infer 3-D structure from biplanar views, but that these vascular detection methods also result in the quantification of the anatomical structure. Thus, the location and quantitative characterization of stenotic segments are obtained simultaneously with their geometrical configuration. Armed with this information, a more accurate and objective visualization becomes possible.

3-D Reconstruction of Vascular Structure

The vascular structure detected in the corrected, 2-D, biplane views represents the basic information on which the 3-D reconstruction of the arterial tree is based. At this point, the principal step is that of backprojection. The backprojection is performed by a recursive traversal of the data structure, which is now completely defined—i.e., no new bifurcations or branches are further introduced. The 3-D reconstruction is accomplished branch by branch as the data structure is traversed, and, at the end of last branch, the reconstructed solution is also stored in the hierarchical data structure and is available for analysis, iterative improvement through user interaction, graphical rendering, or output.

The traversal of the data structure begins at the root bifurcation, which corresponds to the starting location of the anatomic structure and is also defined during the manual selection process. Branches are reconstructed by backprojecting the center points through the isocenter back to the source. As the entire branch is defined, the center points determine the length and path taken by the vessel, while the edges estimate the widths of the vessel. As the backprojection is performed, 3-D coordinate information is calculated and the resulting 3-D reconstruction stored. If there is a bifurcation at the end of the branch, the next level of recursion is invoked to traverse and reconstruct all of the branches under that bifurcation. When all of the branches under a given bifurcation have been reconstructed, the program returns to the next higher level of recursion, and proceeds to reconstruct the next branch at that bifurcation. This procedure is repeated until the entire data structure is traversed and the backprojection routine ends. At present, the operator decides how many branches are reconstructed and to what degree of vasculature the reconstruction is to be performed (current emphasis is on first-order branches).

As previously pointed out, there are numerous shortcomings associated with reconstructions based on backprojection from limited views. One result of these shortcomings is that the backprojection lines will almost certainly not yield the true solution—in fact, backprojection lines corresponding to the same point in two different views will most likely not intersect each other, as illustrated in Fig. 4. A practical solution to this problem can be obtained by solving for the point in 3-D space which minimizes the distance between the backprojected lines: referring to Fig. 4 once again, the estimated solution point can be defined as the midpoint of the line segment Δ. This estimate can be calculated for all backprojection line pairs, thereby generating a set of coordinate triplets for vessel center points. The procedure for reconstructing a single point P can be summarized and generalized for N views thus: Give N views $\{V_1 \cdots V_N\}$, assume the corresponding X-ray source positions $\{S_1 \cdots S_N\}$ and corresponding projection points $\{P_1 \cdots P_N\}$ on the image planes of V_1 through V_N are known. Then, define the set of parametric lines $\{L_1 \cdots L_N\}$ which connect the source points and projected points, as in (1) below:

$$L_j = S_j + t_j\,(S_j - P_j), \qquad \text{for } j = 1, \cdots, N \quad (1)$$

where L_j = projection line from S_j to P_j, S_j = 3-D position of X-ray source for jth image, P_j = 3-D projected point on jth image, and t_j = scalar parameter for jth projection line. The backprojected solution is computed by finding the set of scalars $\{t_1, \cdots, t_N\}$ which minimize the sum of the squared distances between the N projection lines,

$$\text{Minimize} \left\{ \sum_{j=1}^{N} \sum_{i=1}^{N} (L_i - L_j)^2 \right\}. \quad (2)$$

The minimum is found by differentiating with respect to t_j and solving the N by N linear system given by the following expression:

$$\begin{bmatrix} D_1 \cdot D_1\,(1-N) & D_1 \cdot D_2 & \cdots & D_1 \cdot D_N \\ D_2 + D_1 & D_2 \cdot D_2\,(1-N) & \cdots & D_2 \cdot D_N \\ \vdots & \vdots & & \vdots \\ D_N \cdot D_1 & D_N \cdot D_2 & \cdots & D_N \cdot D_N(1-N) \end{bmatrix} \begin{bmatrix} t_1 \\ t_2 \\ \vdots \\ t_N \end{bmatrix} = \begin{bmatrix} \sum_{i=1}^{N} (S_1 - S_i) \cdot D_1 \\ \sum_{i=1}^{N} (S_2 - S_i) \cdot D_2 \\ \vdots \\ \sum_{i=1}^{N} (S_n - S_i) \cdot D_N \end{bmatrix} \quad (3)$$

where $D_j = (S_j - P_j)$ for $j = 1, \cdots, N$. The solution set of the linear system $\{t_1, \cdots, t_N\}$ defines N points on the N projection lines which minimize the squared distance sum in (2). The centroid of these N points is selected as the backprojected 3-D solution point:

$$\text{Centroid} = \frac{\sum_j [S_j + t_j(S_j - P_j)]}{N}. \quad (4)$$

Associated with this solution is the root mean squared distance between the solution point and the N points on the N projection lines corresponding to the N parametric solutions $\{t_1, \cdots, t_N\}$:

$$\Delta' = \sqrt{\frac{1}{N}\sum_{j=1}^{N} \left\{\text{Centroid} - [S_j + t_j(S_j - P_j)]\right\}^2}. \quad (5)$$

The value of the term of (5) may be interpreted as a measure of the degree to which the two images used in backprojection are "aligned" (or misaligned) with each other, in the form of a backprojection discrepancy. It is noteworthy that other authors set this backprojection discrepancy to zero [20], effectively forcing the backprojection lines to intersect to yield a single solution point.

To quantify and visualize the actual locations and dimensions of the vascular structure, the location of vessel center points and the dimensions of corresponding radii (radii that describe the circular lumen or "slice" cross section), must be determined. The radii and the orientation of the slices are determined, in turn, by the edge widths and the orientation of the vessel centerline. As previously mentioned, these widths and orientation values are obtained from detection of the structure in 2-D, and are subsequently mapped onto 3-D coordinates of the reconstruction system by using image orientation and descriptor vectors calculated during geometrical transformations that map 2-D image coordinates in to 3-D coordinates of the projected point based on rotation and skew angles and on the distance to the image intensifier; two 3-D direction vectors define the slice orientation at every center point.

Visualization of Anatomic Information

The data that comprise the visualization information consist of reconstructed 3-D solution points, as well as the entire 2-D and 3-D information, all of which is stored in the hierarchical data structure. These data are presented in two forms, visually and textually: both as a graphical, geometric model describing the 3-D reconstruction solution, and as a summary describing the quantitative arterial information [dimensions, locations of various sites, and backprojection discrepancies of the form of (5)]. Further interaction is possible at this stage between the visual model and the user.

For visualization, a computer model of the arterial structure is generated and rendered. A geometric modeling software package, developed at Georgia Tech and called MAX [32], is used to represent the reconstructed 3-D models. The data structure, however, has been designed to be easily modified in order to support other formats, for instance, the format of the Wavefront Technologies Imaging System [33]. The current model description is based on a generalized truncated frustum. As shown in Fig. 8, this is a singularly curved surface connecting two elliptical ends, although the assumption of circular ends is made [19]. The arterial structure is thus represented by a continuous set of these generalized frusta connecting the branch centers, as depicted in Fig. 8. (Other geometric primitives besides cone frusta are available, such as flat plates, hermite patches, ellipsoids, and toroids; hermite patches are used to model the myocardium, as described in the next section). Bifurcations are formed by connecting the first slice in a branch to the last slice in the branch from which the bifurcation is made, where a slice is defined by the centerpoint of the vessel, a radius value for the circular lumen of the vessel, and two direction vectors defined in the plane in which the cross section lies. The generalized frustum is defined by the surface connecting two arbitrarily oriented elliptical ends. The reconstructed arteries are modeled as connected frustal segments with circular ends. In the general case, each elliptical end of a frustum is defined by three vectors: a center point and two axes. The center point is a position vector describing and endpoint of the frustum, while the two axes are direction vectors which describe the orientation of the frustum's end. The magnitudes of the axes represent the major and minor axes of the elliptical end. Start and stop angles de-

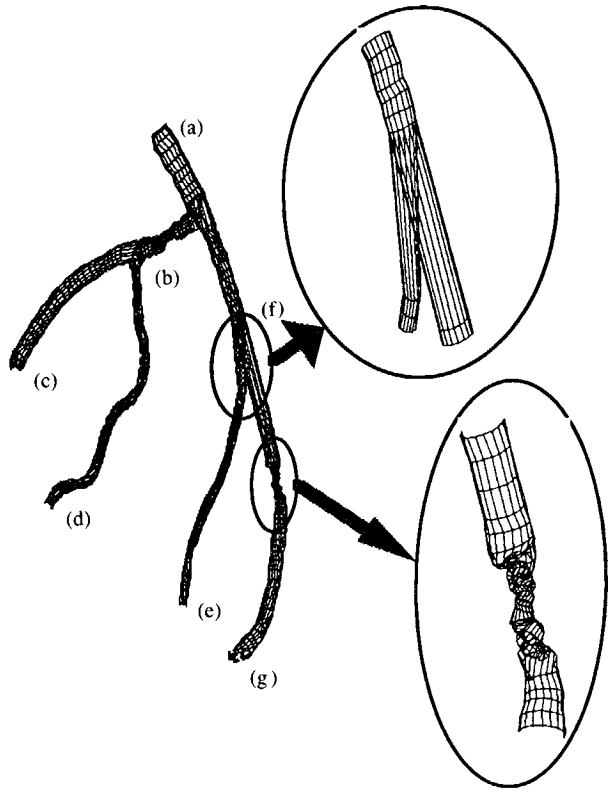

Fig. 8. 3-D wire-frame model of the phantom's arterial structure. Enlarged sections illustrate details of the bifurcation and stenotic site. Labels (a)–(g) represent sites used in measuring segment lengths for error analysis.

fine arcs on each elliptical end, and the generalized frustum is the surface which connects the arcs on both ends. On each elliptical end, the start and stop angles are measured from the first axis vector defining the ellipse, to the second axis vector defining the ellipse. These angles, and the arc that lies between them, are determined by the right-hand convention using the two axis vectors. Frusta are displayed as a collection of quadrilateral plates connecting equally spaced (in angle) points along the two arcs on the frustum's ends.

The arterial reconstruction procedure creates a MAX command file describing the geometry and structure of the vessels. Once this file is read, the entire vasculature, or any subsets of branches and bifurcations, can be displayed from arbitrary viewpoints. This ability to view arterial structure from any orientation provides a significant visualization advantage over being constrained to limited sets of views, such as those of Fig. 2. In addition, the models may be displayed as simple wireframes (as in Fig. 8) or as shaded surfaces using either assigned model colors or arbitrarily reassigned colors. Shaded models enhance the 3-D appearance of the structure, thereby facilitating the clinical assessment of the arteries. In shaded renderings, the Gouraud [34] algorithm is used to interpolate color shades across individual polygons based upon colors computed at the vertices to provide continuous and smoother color changes across curved surfaces. The colors at the vertices are computed from vertex normal vectors and the position of a specified light source.

The results obtained with a copper-wire phantom and with a patient study are shown in Figs. 9 and 10, respectively. In each case, the results are shown to illustrate visualization of the original structure next to the reconstructed structure. Qualitatively, 3-D visualization seems to enable the viewer to distinguish different branches and perhaps also discern the relative orientations and "directions" of the different branches. In addition, the ensemble of 3-D information as a whole provides an intuitive sense of a patient's gross coronary structure, suggesting overall size and perfusion characteristics. Perhaps most importantly, the vascular structure can be visualized from any desired angle, which can be provided useful insights to support the clinical decision-making process, especially regarding possible courses of therapy to treat stenotic lesions.

Major advantages of the 3-D model are that it provides quantitative information for objective evaluations, and that the vascular structure can be rotated, illuminated, and visualized at any desired orientation. Some disadvantages are that not all levels of vasculature can be easily represented, and that a loss in the intrinsic resolution of angiographic data has occurred due to digitization, processing, etc. Ultimately, it may prove more clinically useful to use both 2-D and 3-D visualizations as complementary sources of information in the decision-making process.

In terms of quantitative characterization of the vascular structure, preliminary error analyses have been conducted to determine the representational accuracy of the visualization methodology. The analyses are based on studies performed with the same copper model of the left coronary artery as shown in Fig. 9. Since the phantom has known radii dimensions, comparisons were made between known actual, dimensions and the corresponding radii dimensions predicted by the 3-D reconstruction methodology. The radius error for the copper wire phantom is defined as

TABLE I
RADIUS ERROR FOR COPPER WIRE PHANTOM

Branch	Measured Radius (mm)	# Reconstructed Radii Used	Mean Radius (mm)	Error e (mm)
Main Branch	2.4	9	2.18	0.259
Proximal Cir.	1.65	21	1.53	0.140
Diag2	1.0	21	0.844	0.164
OM1	1.0	49	0.971	0.101
Prox. LAD	1.65	15	1.45	0.202
Distal Cir.	1.65	26	1.60	0.078

$$e = \sqrt{\frac{1}{N}\sum_{i=1}^{N}(R_i - R_m)^2} \tag{6}$$

where R_i is the reconstructed (predicted) radius and R_m is the measured (actual) radius at a particular point in the phantom. As indicated in Table I, the radius was measured once for each of the six branches. For each of these six branches, several radii were calculated along the branch during the reconstruction process, and a mean radius and corresponding error were obtained from the calculated radii. As can be seen from Table I, the error associated with estimating radii for the phantom is on the order of a small fraction of a millimeter. These encouraging preliminary findings serve to confirm the viability of the visualization approach, capable of providing quantitative assessment of the 3-D information. This capability, coupled to the ability to provide a visual rendering of the structure in 3-D, offers the potential to significantly aid in locating and characterizing the extent and severity of CAD.

III. Quantification and Visualization of Physiological Information

Techniques in quantitative myocardial tomography are described in detail elsewhere [14], [35], and the discussions that follow are only intended to include aspects of these techniques which help to clarify the visualization of the integrated modalities.

Tomographic Acquisition and Extraction of Myocardial Perfusion Distribution

Tomographic acquisition of myocardial thallium-201 perfusion studies in patients consist of obtaining 32 projections over a 180° arc [36]. The projections are filtered prior to backprojection using a Hanning Filter with a cut-off frequency of 0.822 cycles/cm. Filtered backprojection is then performed to reconstruct the transverse axial

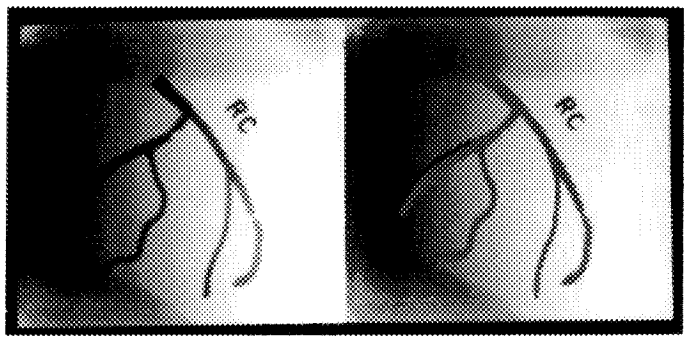

(a) (b)

Fig. 9. Visualization of reconstructed 3-D model of the phantom structure: (a) original image and (b) 3-D model superimposed on original image (a).

(a) (b)

Fig. 10. Visualization of reconstructured 3-D model of a patient's vascular structure: (a) original angiogram and (b) 3-D model superimposed on image (a).

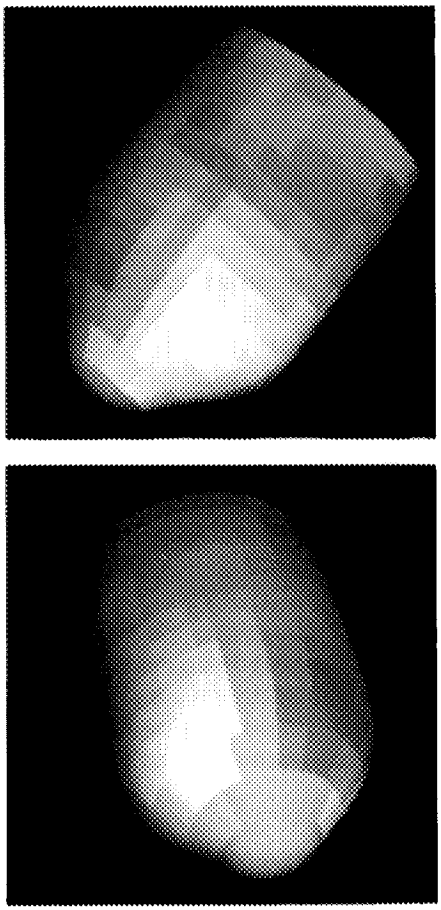

Fig. 11. Visualization of perfusion distribution for phantom from two different viewing perspectives.

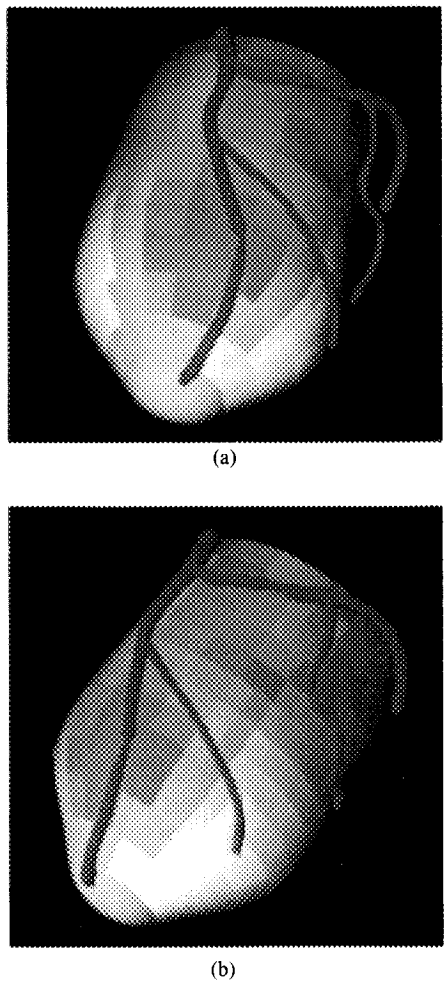

(a)

(b)

Fig. 12. Visualization of unified anatomical and physiological information in two different viewing perspectives (a) and (b).

tomograms, each 6.25 mm thick, encompassing the entire heart. Oblique tomograms parallel to the vertical long and short axes of the left ventricle are extracted from the reconstructed transaxial tomograms by performing a coordinate transformation with appropriate interpolation [37]. Fig. 3 is representative of tomographic slices. A color code is used such that "brighter" colors (e.g., yellow and orange) correspond to relatively higher perfusion distribution levels, while "darker" colors (e.g., blue and purple) correspond to relative hypoperfusion. The short-axis slices to be quantified are selected by an operator following a strict protocol [35]; approximately 12 slices are obtained from a normal-sized heart. For each short-axis slice, the maximal count circumferential profiles (CPs) are then generated automatically for each slice, from the most apical to the most basal slice. Each circumferential profile consists of a set of maximal counts per pixel along a radius extending from the center of the LV to the limit of the radius of search [35].

Visualization of Myocardial Perfusion

The radii of each extracted circumferential profile is filtered in both depth and angle using a 3 × 3, low-pass filter kernel. The filtered radii for each slice are subsequently fit to circles using singular-value decomposition. The visualization model of the myocardial perfusion is built using hermite patches which are surface primitives in the geometric model-generating software MAX [14]. The hermite patch consists of four vertices with a normal vector at each vertex. The hermite patch passes through the four vertices and forms a cubic spline surface defined by the vertices and the vertex normals. The points on the patch surface are found by interpolating the vertex normals and fitting a cubic polynomial through the adjacent points and the interpolated normal vectors. One hermite patch is created for each of the maximal-count CP points on each slice, with vertices and vertex normals based on the fitted radii of the slice under consideration and the slice above it. The apex is modeled as an ellipsoid with x and y radii such that there is a smooth transition between the apex and the first slice, and z radius such that the thickness of the apex is not any greater than the predefined slice thickness. Each patch is assigned a color based on the counts in the associated profile point.

The information resulting from this procedure is employed to render a 3-D surface model of the myocardial perfusion in the form of twenty projections, each 512 × 384 in size, over 360°. Fig. 11 shows the results of this visualization methodology for a phantom (an activity-filled cavity constructed with plastic and shaped in the form of an ellipsoid conforming to the copper-wire arterial structure of Fig. 9). As with the visualization model of arterial structure, the visualization model of perfusion distribution can be rotated, illuminated, and viewed as desired by the operator. This 3-D presentation accomplishes important goals. First, the visualization methodology overcomes the important difficulty associated with visualizing the information contained in multiple tomographic slices, which are inherently three-dimensional but can normally be viewed only as a series of 2-D slices (as many as 52 images!) [14] or by forcing the information into the form of polar plots [35]. More importantly, the interpretive and decision-making process may be greatly enhanced through this visualization approach since the 3-D information is represented in a fashion that more naturally conveys the physiology of interest.

IV. Visualization of Unified Anatomical and Physiological Information

The 3-D coronary arterial tree is registered onto the rendered 3-D myocardial perfusion model in order to visualize both anatomic and physiologic information. Having already discussed the methodologies associated with quantifying and visualizing the information obtained from each modality, this section briefly describes the methodology designed to present the integrated information. In keeping with the goal of emphasizing both subjective as well as objective aspects of the methodology, the discussion will be limited to results obtained with the phantom study since at present this represents the only nontrivial structure (of known and measurable internal dimensions) that has been quantified.

In general, computer graphic tools play a crucial role in the visualization of the unified heart model. As previously discussed, both models are based upon very simple geometric primitives: the coronaries are represented by conical frusta, and the myocardium is represented by hermite patches. The models can be displayed together or separately, as wireframe drawings or shaded renderings, in full color or monochrome, and a particularly useful presentation is made through the use of computer animation. Wireframe drawings are used for quick viewing of the arterial geometry, but shaded renderings provide the best displays for evaluating the patient data. Hidden surfaces are illuminated by maintaining a depth buffer, and a Gouraud shading algorithm with one light source is used to render the polygonal surface elements.

The size and orientation of the elements are determined by the features extracted from the original X-ray and nuclear images. Assumptions about continuity of surfaces and slopes were imposed to provide a more natural display. For example, the conical segments were forced to match the adjacent segments at each end. Our first model employed right cone frusta (with ends orthogonal to the axis), and the discontinuities between the segments along the arterial branches created the misleading visual effect of coronary defects. This problem was overcome by using a generalized cone frustum which allowed nonparallel, nonorthogonal ends. With this new segment type, the frustum ends of adjacent segments were forced to be the same and thereby ensure surface continuity.

The systems used for this research include a SUN 3/260 workstation, PIXAR Image Computer, along with a BARCO high resolution display device. The PIXAR-1 Image Computer has been used primarily to produce animation. The model is rendered at different orientations and a sequence of these stored images is redisplayed rapidly on the PIXAR. Qualitatively, it seems that a full 360° rotation of the heart about the axis of the body provides the best visualization.

Landmarks and Transformations Used for Multimodality Registration

The registration consists of a two-step process: gross and fine alignment. The procedure is best illustrated with the example of human anatomy, although the results presented here are obtained with the phantom model previously described. After appropriate scaling of imaging modalities, registration in 3-D consists of a gross alignment using the same approximate degrees of freedom available to both imaging modalities. Specifically, this requires that the orientation of the long axis of the LV remain the same with respect to both detectors' frames of reference (e.g., the patient facing in the same direction for both perfusion

and angiographic studies). This is easily accomplished for the case of the phantom model.

Gross alignment is followed by a fine alignment procedure, as follows. The proximal length of the left anterior descending (LAD) artery, as well as the posterior descending branch of the right coronary artery (RCA) follow interventricular grooves which are easily identified from myocardial perfusion studies. Thus, initial registration can be guided by superimposing the major coronary vessels on these grooves, which can be previously identified from the myocardial short-axis slices. Since information is obtained independently for the RCA and LAD vessels during the angiographic procedure, this superimposition can be done independently for each branch. Following the pattern of these naturally occurring landmarks, a 1 cm-thick rounded plastic chamber was used to simulate the anterior myocardial wall of the right ventricle in order to provide a fiducial landmark to align the copper-wire model of the left coronary arterial tree. Currently, the 3-D rotations and translations are performed on a case-by-case basis: given the relative orientations and positions associated with each study for both imaging modality, the inverse rotations and translations necessary for alignment are calculated manually. In addition, using the hierarchical data structures, interactive manipulation of both 3-D models (i.e., the models describing anatomic and physiologic information) is possible.

Visualization of Unified Model

The unified visualization model is displayed in Fig. 12. Fig. 12(a) and (b) present the unified anatomical and physiological information from two different viewing perspectives. As before, visualization is possible from any desired, user-definable illuminations, rotations, and magnification specifications.

Animated displays are also possible by specifying different combinations of these parameters in conjunction with various display rates. This presentation of the integrated information allows for quickly visualizing whether any correlations might exist between structure (in particular, stenotic lesions) and function (particularly hypoperfusion). In addition to presenting a significant amount of multimodality information in a single visualizable presentation, it should be stressed that, as previously discussed, the methodology is also designed to quantify the displayed information, such as the dimensions of stenotic lesions. To further aid in decision-making, the methodology can also provide information both visually and textually. Hence, both objective and subjective assessments are possible in complementary forms. The overall advantage, however, is that the physician is no longer required to view large numbers of 2-D images separately, or expected to make subjective estimates of vital structural and functional parameters. It is expected that this type of comprehensive, unified approach should lead to improvements in the medical decision-making process by providing both quantitative and qualitative information in an interactive, systematic, and meaningful manner.

V. Summary and Future Directions

A methodology for quantifying and visualizing multimodality cardiac imagery has been presented. The methodology combines numerous unique elements: 1) a hierarchical data structure that organizes information and logical procedures in a natural fashion while at the same time support user interaction with the data: 2) knowledge-based techniques for detecting and locating vascular structure from angiographic images in a partially automated fashion; 3) representation of actual geometry inherent in X-ray biplane angiography rather than (source-at-infinity) parallel geometry; 4) calculation of absolute errors (between phantom models of known dimensions and dimensions computed from the reconstructed models); 5) quantification and visualization of vascular structure, including estimates of vessel widths; 6) quantification and visualization of myocardial function, including estimates of perfusion distribution levels in the left ventricular myocardium; and 7) quantification and visualization model of the integrated anatomical and physiological information. The visualization methodology was implemented with phantom and patient studies, showing the viability of the approach for both quantitative and qualitative interpretations of multimodality imagery in nontrivial cases. The visualization of the unified multimodality information is shown in Fig. 12, which illustrates the presentation of very large amounts of data in a meaningful, succinct, and natural fashion. This figure should be compared with Figs. 2 and 3, which present the same information from both imaging modalities but using current visualization methods.

The preliminary findings produced encouraging results, while also providing considerations for further investigation. The entropy operator used in the detection of vessel edges yielded good results, which were corroborated through comparisons with the known dimensions of a copper-wire phantom model. However, additional anatomically-based knowledge is required for guiding the detection procedure, especially in handling vessel thinning or widening, and where vessel bifurcations and overlaps occur. In terms of registration of the different imaging modalities, the methodology and associated phantom results showed good agreement in terms of conveying the unified anatomic and physiologic information. Techniques are being developed to generalize the 3-D transformations required for consistent registration of any given set of multimodality imagery.

The thrust of current efforts is two-fold: a) increased automation of the entire visualization methodology to reduce operator workload and b) continued testing of the accuracy and reliability of the methodology. With respect to automation of the procedure, the goal is to develop knowledge-based methods to effect the limited-view reconstruction of arterial structure. Testing procedures will rely on the development and implementation of phantoms and patient studies to determine possible sources of errors, particularly in the areas of backprojection and reconstruction.

The visualization methodology that has been presented is designed to convey a significant amount of multimodality information in a single, meaningful display. The methodology is also designed to quantify the visualized information, and to provide the information both visually and textually. Hence, both objective and subjective assessments of medical information are possible in complementary forms and in interactive fashions. It is expected that this type of comprehensive, unified approach to visualization should lead to improvements in the accuracy and reliability of patients' diagnosis, prognosis, and selection of therapeutic courses of action, thereby facilitating the medical decision-making process in an important problem in health-care.

REFERENCES

[1] P. Harris, D. Phil, F. E. Harrell, K. L. Lee, V. S. Behar, and R. A. Rosati, "Survival in medically treated coronary artery disease," *Circulation*, vol. 60, pp. 1259–69, 1979.

[2] G. S. Roubin, P. J. Harris, L. Bernstein, and D. T. Kelly, "Coronary anatomy and prognosis after myocardial infarction in patients 60 years and younger," *Circulation*, vol. 67, p. 743, 1983.

[3] G. S. Roubin, W. F. Shen, D. T. Kelly, and P. J. Harris, "The *QRS* scoring system for estimating myocardial infarct size: Clinical, angiographic and prognostic correlations," *J. Amer. Coll. Cardiol.*, vol. 2, p. 38, 1983.

[4] H. Dash, R. A. Johnson, R. E. Dinsmore, and J. W. Harthorne, "Cardiomyopathic syndrome due to coronary artery disease: Relation to angiographic extent of coronary disease and to remote myocardial infarction," *Brit. Heart J.*, vol. 39, pp. 733–739, 1977.

[5] J. O. Humphries, L. Kuller, R. S. Ross, G. C. Friesinger, and E. E. Page, "Natural history of ischemic heart disease in relation to arteriographic findings. A twelve year study of 224 patients," *Circulation*, vol. 49, pp. 489–497, 1974.

[6] I. Ringquist, L. D. Fisher, M. Mock, K. B. Davis, H. Wedel, B. R. Chaitman *et al.*, "Prognostic value of angiographic indices of coronary artery disease from the coronary artery surgery study (CASS)," *J. Clin. Invest.*, vol. 71, pp. 1854–66, 1983.

[7] K. L. Gould, "Assessing coronary stenosis severity: A recurrent clinical need," *JACC*, vol. 8, pp. 91–94, 1986.

[8] G. M. Pohost, L. M. Zir, R. H. Moor *et al.*, "Differentiation of transiently ischemic from infarcted myocardium by serial imaging after a single dose of Tl-201," *Circulation*, vol. 55, p. 294, 1977.

[9] F. G. Wackers, E. B. Sokole, G. Samson *et al.*, "Value and limitations of thallium-201 scintigraphy in the acute phase of myocardial infarction," *New Eng. J. Med.*, vol. 295, p. 1, 1976.

[10] F. X. Pamelia, G. G. Craddock, D. D. Watson, R. S. Gibson, J. Sirowatka, and G. A Beller, "Outcome and prognosis of patients with chest pain and normal thallium-201 exercise scans," *Circulation*, vol. 64, p. 34, 1981.

[11] H. Staniloff, G. Diamond, J. Forrester, D. Berman, and H. J. C. Swan, "Prediction of death infarction," *Amer. J. Cardiol.*, vol. 49, p. 967, 1982.

[12] S. Mousa, J. Cooney, and S. Williams, "Regional myocardial distribution of RP-30 in animal models of myocardia ischemia and reperfusion," *J. Nucl. Med.*, vol. 28, p. 620, 1987.

[13] C. D. Cooke, L. Jofre, L. Klein *et al*, "3D reconstruction of arterial structure from biplane angiography," in *Proc. IEEE Technicon*, Miami, FL, Oct. 1987.

[14] E. G. DePuey, E. V. Garcia, and N. F. Ezquerra, "3D techniques and artificial intelligence in Thallium-201 cardiac imaging," *Amer. J. Roentgenol.*, vol. 152, p. 1161–1168, June 1989.

[15] N. F. Ezquerra, M. Zerbi, D Cooke, J. W. Peifer, M. S. West, G. J. Bradley, L. Jofre, J. L. Klein, H. L. Hise, and E. V. Garcia, "A method for 3D display of arterial structure superimposed on myocardial perfusion distribution," *J. Nucl. Med.*, vol. 28, no. 4, pp. 675–676.

[16] R. H. Selzer, D. H. Blankenhorn, D. W. Crawford, S. H. Brooks, R. Brandt, Jr., "Computer analysis of cardiovascular imagery," in *Proc. Cal Tech FPL Conf. Image Process. Technol., Data Sources Software Commercial Scientific Appl.*, Pasadena, CA, California Inst. Tech., 1976, pp. 1–20.

[17] J. R. Spears, T. Sandor, A. V. Als, M. Malagold, J. E. Markis, W. Grossman, J. R. Serur, and S. Paulin, "Computerized image analysis for quantitative measurement of vessel diameter from cineangiograms," *Circulation*, vol. 68, p. 453, 1983.

[18] R. L. Kirkeeide, P. Fung, R. W. Smalling, and K. L. Gould, "Automated evaluation of vessel diameter from arteriograms," *Comput. Cardiol.*, Long Beach, CA, IEEE Computer Society, 1982, pp. 215–218.

[19] K. Kitamura, J. M. Tobis, and J. Sklansky, "Estimating the 3-D skeletons and traverse areas of coronary arteries from biplane angiograms," *IEEE Trans. Med. Imaging*, vol. 7, no. 3, Sept. 1988.

[20] J. Barba, P. Fenster, M. Suardiaz, and K. K. Wong, "3D arterial traces from biplane projections," *SPIE Med. Imaging*, vol. 767, 1987.

[21] "Mol CR: 3D reconstruction from biplane x-ray angiography," Tech. Rep. IBM UK Scientific Center, Sept. 1984.

[22] D. R. Smith, G. P. Robinson, J. M. Burriage, and P. Quarindon, "Quantitative moving three-dimensional images of the heart and coronary arteries: An automated method of production," *Circulation*, vol. 74, 1986.

[23] P. Fornster, J. Barba, M. Suardiaz *et al.* "Arterial cross-section reconstruction from bi-plane x-ray shadowgraphs," *SPIE Med. Imaging*, vol. 767, pp. 433–440, 1987.

[24] R. A. Kruger and S. J. Rieder, *Basic Concepts of Digital Substraction Angiography*. Princeton, NJ: G. K. Hall, 1984.

[25] J. E. Bresenham, "Algorithm for computer control of a digital plotter," *IBM Syst. J.*, vol. 4, 1, pp. 25–30, 1965.

[26] C. J. Kooijam, J. H. C. Reiber *et al.* "Computer-aided quantization of the severity of coronary obstructions from single view cineangiograms," *Proc ISMII*, vol. 82, p. 59, 1982.

[27] J. H. C. Reiber, J. J. Gerbrands *et al.* "3-D reconstruction of coronary arterial segments from two projections," *Digital Imaging Cardiovasc. Radiol., Intern Symp. Kiel*, 1982, P. H. Heintzen and R. Brenneke, Eds. New York: Georg Thieme Verlag, Stuttgart, pp. 151–163.

[28] W. K. Pratt, *Digital Image Processing*. New York: Wiley, 1978.

[29] E. L. Hall, *Computer Image Processing and Recognition*. New York: Academy, 1979.

[30] A. Shiozaki, "Edge extraction using entropy operator," *Comput. Vis., Graph., Image Process.*, vol. 36, pp. 1–9, 1986.

[31] J. Canny, "A computational approach to edge detection," *IEEE Trans. Pattern Anal. Mach. Intell.*, PAMI-8, no. 6, 1986.

[32] J. W. Peifer, M. S. West, and R. B. Rakes, "MAX geometric data base editor user's manual, rev. 5.0," GTRI, Georgia Inst. Technol., Atlanta, GA, 1987.

[33] Wavefront Technologies 3D Dynamic Imaging System, Wavefront Technologies, Inc., Santa Barbara, CA.

[34] H. Gouraud, "Computer display of curved surfaces," U. Utah Comp. Science Dep., UTEC-CSc-71-113, June 1971; NTIS AD-762 018; abridged version in *IEEE Trans. Comput.*, vol. C-20, p. 623, June 1971.

[35] E. V. Garcia, E. G. DePuey, and E. E. Pasquale, "Quantitative planar and tomographic Thallium-201 myocardial perfusion imaging," *Cardiovasc. Intervent. Radiol.*, vol. 10, pp. 374–383, 1987.

[36] D. L. Williams, J. L. Ritchie, G. D. Harp, J. H. Caldwell, G. W. Hamilton, R. L. Eisner, and D. J. Nowak, "Preliminary characterization of the properties of a transaxial whole-body single-photon tomograph: Emphasis on future application to cardiac imaging in Functional mapping of organ systems," in *Society of Nuclear Medicine*, P. D. Esser, Ed. 1981, p. 149.

[37] J. A. Borello, N. H. Clinthorne, W. L. Rogers, J. H. Thrall, and J. Keyes, "Oblique-angle tomography: A restructuring algorithm for transaxial tomographic data," *J. Nucl. Med.*, vol. 22, pp. 471–473, 1981.

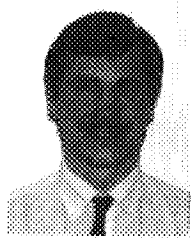

John W. Peifer (M'88) was born in Austin, MN, on October 12, 1954. He received the B.S. (magna cum laude) and the M.A. degrees in mathematics from the University of Georgia, Athens, in 1976 and 1977, respectively.

He worked as a Research Scientist in the Modeling and Analysis Division of the Radar and Instrumentation Laboratory at the Georgia Tech Research Institute in Atlanta, GA from 1977 through 1988. Currently, he is a Senior Research Scientist in the Bioengineering Center at the Georgia Institute of Technology, Atlanta GA. His research interests are in computer modeling, graphics, and medical imaging.

Norberto F. Ezquerra was born in Santa Clara, Cuba, February 21, 1949. He received the B.S. degrees in mathematics and physics from the University of South Florida, Tampa, and the M.S. and Ph.D. degrees in elementary particle physics and fields from Florida State University, Tallahassee, in 1974 and 1978, respectively.

In 1978 he joined the research faculty at Georgia Institute of Technology, Atlanta, where he served as Senior Research Scientist in the Georgia Tech Research Institute. In 1985 he joined the Bioengineering Center of the Office of Interdisciplinary Programs, where he is currently Director of the Medical Informatics Laboratory. He is active in various areas of medical informatics, including artificial intelligence, computer vision, and visualization in medicine.

Dr. Ezquerra is the recipient of an NIH FIRST Award from the National Library of Medicine to investigate the application of artificial intelligence methods to cardiovascular imaging. He is a member of IEEE Computer Society, American Medical Informatics Association, American Physical Society, IEEE EMBS, Sigma Xi, American Association of Physics Teachers, and American Association for the Advancement of Science.

Charles David Cooke was born in Atlanta, GA, on August 5, 1963. He received the B.E.E. degree from Auburn University, Auburn, AL, in 1986 and the M.S.E.E. degree from the Georgia Institute of Technology, Atlanta, in 1987.

In 1988, he joined the faculty of the Emory University School of Medicine in Atlanta, GA. His current research interests include medical image processing, volume and surface rendering, and the application of artificial intelligence to medical images.

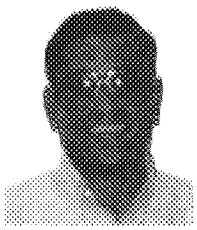

Rakesh Mullick (S'87) was born in Poughkeepsie, NY, on November 26, 1966. He received the B.S. degree electrical engineering from the University of Rochester, Rochester, NY, in 1988.

He is currently pursuing the Ph.D. degree in electrical engineering at the Georgia Institute of Technology where he is a graduate research assistant. His current interests are in image processing, pattern recognition and high-speed DSP.

Mr. Mullick is a member of Tau Beta Pi, Phi Beta Kappa, and of the IEEE ASSP society.

L. Klein, photograph and biography not available at the time of publication.

M. Eric Hyche was born in Kingsport, TN, on July 24, 1965. He received the B.S. degree in electrical engineering from Tennessee Technological University, Cookeville, in 1987 and the M.S. degree in electrical engineering, from the Georgia Institute of Technology, Atlanta, in 1989. He is currently pursuing the Ph.D. degree in electrical engineering at the Georgia Institute of Technology, where he is a graduate fellow of the Office of Naval Research.

Mr. Hyche is a member of Eta Kappa Nu, Tau Beta Pi, and Phi Kappa Phi.

Ernest V. Garcia (M'83) was born in Havana, Cuba, on September 14, 1948. He received his B.S., M.S., and Ph.D. degrees from the University of Miami, Florida, in 1971, 1972, and 1974, respectively.

In 1974 he joined the faculty at the University of Miami where he served as Assistant and Associate Professor of Radiology. In 1979 he joined Cedars-Sinai Medical Center in Los Angeles where he stayed until 1985 as Director of Medical Imaging Physics. He is currently Professor of Radiology at Emory University, Atlanta, Georgia. He has authored or coauthored over 120 manuscripts and chapters in the fields of nuclear medicine, cardiovascular imaging and image processing. He is a member of the editorial board of the *American Journal of Cardiovascular Imaging*, the *International Journal of Cardiovascular Imaging*, and the journal of *Nuclear Medicine Communications*.

Dr. Garcia is a member of the Society of Nuclear Medicine and the American Heart Association.